

## CO( $J=1\rightarrow 0$ ) IN $Z>2$ QUASAR HOST GALAXIES: NO EVIDENCE FOR EXTENDED MOLECULAR GAS RESERVOIRS

DOMINIK A. RIECHERS<sup>1</sup>, CHRISTOPHER L. CARILLI<sup>2</sup>, RONALD J. MADDALENA<sup>3</sup>, JACQUELINE HODGE<sup>4</sup>, ANDREW I. HARRIS<sup>5</sup>,  
ANDREW J. BAKER<sup>6</sup>, FABIAN WALTER<sup>4</sup>, JEFF WAGG<sup>7</sup>, PAUL A. VANDEN BOUT<sup>8</sup>, AXEL WEISS<sup>9</sup>, AND CHELSEA E. SHARON<sup>6</sup>

*draft version October 23, 2018, accepted for publication in the Astrophysical Journal Letters (EVLA Special Issue)*

### ABSTRACT

We report the detection of CO( $J=1\rightarrow 0$ ) emission in the strongly lensed high-redshift quasars IRAS F10214+4724 ( $z=2.286$ ), the Cloverleaf ( $z=2.558$ ), RX J0911+0551 ( $z=2.796$ ), SMM J04135+10277 ( $z=2.846$ ), and MG 0751+2716 ( $z=3.200$ ), using the Expanded Very Large Array and the Green Bank Telescope. We report lensing-corrected CO( $J=1\rightarrow 0$ ) line luminosities of  $L'_{\text{CO}} = 0.34\text{--}18.4 \times 10^{10} \text{ K km s}^{-1} \text{ pc}^2$  and total molecular gas masses of  $M(\text{H}_2) = 0.27\text{--}14.7 \times 10^{10} M_{\odot}$  for the sources in our sample. Based on CO line ratios relative to previously reported observations in  $J \geq 3$  rotational transitions and line excitation modeling, we find that the CO( $J=1\rightarrow 0$ ) line strengths in our targets are consistent with single, highly-excited gas components with constant brightness temperature up to mid- $J$  levels. We thus do not find any evidence for luminous extended, low excitation, low surface brightness molecular gas components. These properties are comparable to those found in  $z>4$  quasars with existing CO( $J=1\rightarrow 0$ ) observations. These findings stand in contrast to recent CO( $J=1\rightarrow 0$ ) observations of  $z \simeq 2\text{--}4$  submillimeter galaxies (SMGs), which have lower CO excitation and show evidence for multiple excitation components, including some low-excitation gas. These findings are consistent with the picture that gas-rich quasars and SMGs represent different stages in the early evolution of massive galaxies.

*Subject headings:* galaxies: active — galaxies: starburst — galaxies: formation — galaxies: high-redshift — cosmology: observations — radio lines: galaxies

### 1. INTRODUCTION

Investigations of the molecular and dusty interstellar medium (ISM) in high redshift galaxies are of key importance to studies of galaxy evolution at early cosmic times, as the ISM provides the material that fuels star formation and stellar mass assembly. It is particularly interesting to better understand the ISM properties of galaxies that host both intense star formation and a luminous active galactic nucleus (AGN), as this enables simultaneous investigations of supermassive black hole and stellar bulge growth in galaxies. A key cosmic epoch for such studies is the redshift range  $2 \lesssim z \lesssim 3$ , where both cosmic star formation and AGN activity peak, and thus, where most of the growth of stellar and black hole mass in galaxies occurs (e.g., Magnelli et al. 2009; Richards et al. 2006).

Some of the most remarkable distant AGN-starburst galaxies are gas-rich, far-infrared luminous quasars at  $z>2$ . To date, the molecular ISM of 34 high- $z$  quasars has been detected through emission from rotational lines of CO, 14 of which are gravitationally lensed (see review by Solomon & Vanden Bout 2005, and Riechers 2011 for a recent summary). Given the sensitivity of past observatories, gravitational lensing is key to probe down to intrinsically fainter (and thus, more common) systems. One key aspect of these studies is that most detections were obtained in mid- $J$  (i.e.,  $J \geq 3$ ) CO transitions. Only three of the 34 quasars were observed in the ground-state CO( $J=1\rightarrow 0$ ) line (e.g., Carilli et al. 2002; Riechers et al. 2006a). It thus remains a possibility that many of these studies are biased toward the highly excited gas that does not necessarily trace the entire molecular gas reservoir seen in CO( $J=1\rightarrow 0$ ).

To overcome the limitations of previous studies, we have initiated a systematic study of the CO( $J=1\rightarrow 0$ ) content of high- $z$  quasars and other galaxy populations with the Expanded Very Large Array (EVLA; Perley et al. 2011) and the 100m Robert C. Byrd Green Bank Telescope (GBT). In this Letter, we report the detection of CO( $J=1\rightarrow 0$ ) emission toward five strongly lensed  $z>2$  quasars, using the EVLA and the GBT. We use a concordance, flat  $\Lambda$ CDM cosmology throughout, with  $H_0=71 \text{ km s}^{-1} \text{ Mpc}^{-1}$ ,  $\Omega_M=0.27$ , and  $\Omega_\Lambda=0.73$  (Spergel et al. 2003, 2007).

### 2. OBSERVATIONS

#### 2.1. EVLA

We observed the CO( $J=1\rightarrow 0$ ) ( $\nu_{\text{rest}} = 115.2712 \text{ GHz}$ ) emission line toward IRAS F10214+4724 ( $z=2.286$ ), the

<sup>1</sup> Astronomy Department, California Institute of Technology, MC 249-17, 1200 East California Boulevard, Pasadena, CA 91125, USA; dr@caltech.edu

<sup>2</sup> National Radio Astronomy Observatory, PO Box O, Socorro, NM 87801, USA

<sup>3</sup> National Radio Astronomy Observatory, P.O. Box 2, Green Bank, WV 24944, USA

<sup>4</sup> Max-Planck-Institut für Astronomie, Königstuhl 17, D-69117 Heidelberg, Germany

<sup>5</sup> Department of Astronomy, University of Maryland, College Park, MD 20742-2421, USA

<sup>6</sup> Department of Physics and Astronomy, Rutgers, the State University of New Jersey, 136 Frelinghuysen Road, Piscataway, NJ 08854-8019, USA

<sup>7</sup> European Southern Observatory, Alonso de Córdova 3107, Vitacura, Casilla 19001, Santiago 19, Chile

<sup>8</sup> National Radio Astronomy Observatory, 520 Edgemont Road, Charlottesville, VA 22903-2475, USA

<sup>9</sup> Max-Planck-Institut für Radioastronomie, Auf dem Hügel 69, D-53121 Bonn, Germany

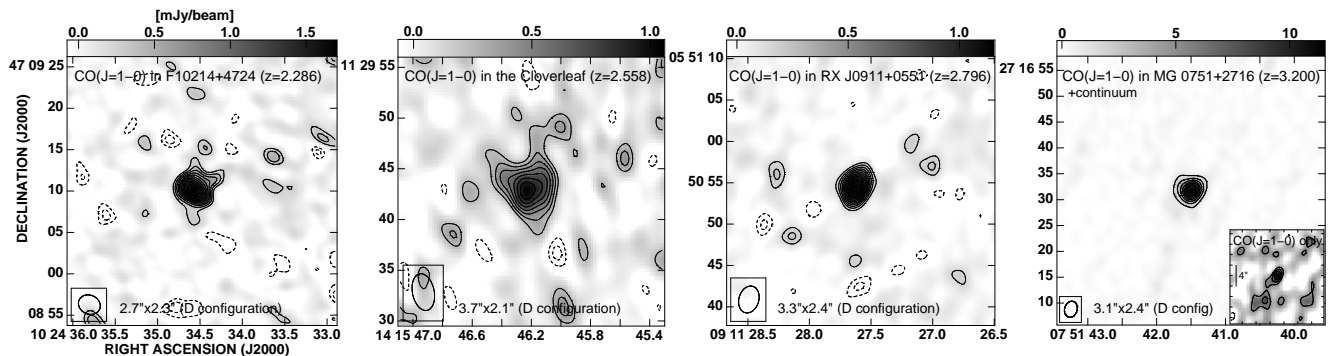


FIG. 1.— EVLA CO( $J=1\rightarrow0$ ) maps of IRAS F10214+4724 ( $z=2.286$ ), the Cloverleaf ( $z=2.558$ ), RX J0911+0551 ( $z=2.796$ ), and MG 0751+2716 ( $z=3.200$ ). The resolution is indicated at the bottom of each panel. For MG 0751+2716, the inset shows the CO line emission after subtracting the underlying continuum emission. Contours are in steps of  $1\sigma=125, 115, 75$ , and  $330\ \mu\text{Jy beam}^{-1}$  for each source, respectively, starting at  $\pm 2\sigma$  (except the CO+continuum map of MG 0751+2716, where contours are in steps of  $4\sigma$ ). The maps are averaged over  $160, 648, 185$ , and  $306\ \text{km s}^{-1}$  ( $18.75, 70, 18.75$ , and  $28\ \text{MHz}$ ), respectively.

Cloverleaf ( $z=2.558$ ), RX J0911+0551 ( $z=2.796$ ), and MG 0751+2716 ( $z=3.200$ ), using the EVLA. At these redshifts, all lines are shifted to the Ka band ( $0.9\ \text{cm}$ ; see Table 1 for redshifted line frequencies). Observations were carried out under good weather conditions in six D array tracks between 2009 October 26 and December 09, and on 2010 July 17 and 18. This resulted in  $5.0, 1.0, 12.0$ , and  $1.0\ \text{hr}$  ( $2.1, 0.6, 5.1$ , and  $0.6\ \text{hr}$ ) total (on-source) observing time for IRAS F10214+4724, the Cloverleaf, RX J0911+0551, and MG 0751+2716, respectively. For IRAS F10214+4724 and RX J0911+0551, an additional  $0.9$  and  $2.3\ \text{hr}$  on source were spent on separate continuum settings. The nearby quasars J0958+4725, J1415+1320, J0909+0121, and J0748+2400 were observed every  $3.5$  to  $7$  minutes for pointing, secondary amplitude and phase calibration. For primary flux calibration, the standard calibrators 3C286 and 3C147 were observed, leading to a calibration that is accurate within  $\sim 10\%$ .

Observations for the Cloverleaf and MG 0751+2716 were carried out with the WIDAR correlator, using two intermediate frequencies (IFs) of  $128\ \text{MHz}$  (dual polarization) each at  $2\ \text{MHz}$  resolution. For the Cloverleaf, the two IFs were overlapped by two channels, centered on the CO line, yielding  $252\ \text{MHz}$  contiguous bandwidth. For MG 0751+2716, one IF was centered on the CO line, and the second IF was centered on the continuum at  $32.046\ \text{GHz}$ .

Observations for IRAS F10214+4724 and RX J0911+0551 (which have narrow CO lines) were carried out with the previous generation correlator, with two  $21.875\ \text{MHz}$  (dual polarization) IFs at  $3.125\ \text{MHz}$  resolution. For IRAS F10214+4724, both IFs were centered on the CO line, yielding  $43.75\ \text{MHz}$  contiguous bandwidth. For RX J0911+0551, one IF was centered on the CO line, and the second IF was centered on the continuum at  $34.3173\ \text{GHz}$ . For these two sources, one third of the on-source time was spent to observe a second frequency setting with two  $50\ \text{MHz}$  continuum IFs offset by  $\pm 150\ \text{MHz}$  from the CO lines, yielding more sensitive constraints on the continuum emission.

For data reduction and analysis, the AIPS package was used. All data were mapped using ‘natural’ weighting. The data result in final rms noise levels of  $125, 115, 75$ , and  $330\ \mu\text{Jy beam}^{-1}$  over  $160, 648, 185$ , and  $306\ \text{km s}^{-1}$  ( $18.75, 70, 18.75$ , and  $28\ \text{MHz}$ ) widths for IRAS F10214+4724, the Cloverleaf, RX J0911+0551,

and MG 0751+2716, respectively. Maps of the velocity-integrated CO  $J=1\rightarrow0$  line emission yield synthesized clean beam sizes of  $2.7''\times 2.3'', 3.7''\times 2.1'', 3.3''\times 2.4''$ , and  $3.1''\times 2.4''$ .

## 2.2. GBT

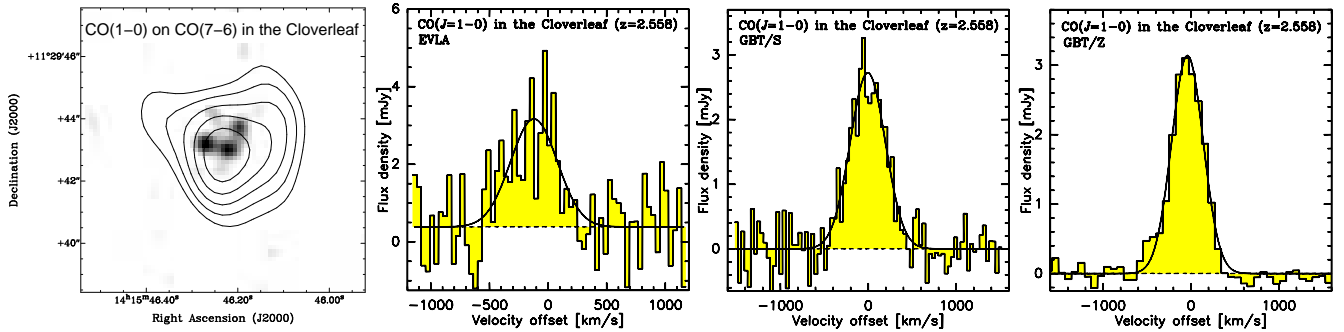
We observed the CO( $J=1\rightarrow0$ ) emission line toward IRAS F10214+4724, the Cloverleaf, SMM J04135+10277 ( $z=2.846$ ), and MG 0751+2716, using the facility Ka band receiver on the GBT with the digital Spectrometer backend (GBT/S) and the Zpectrometer analog lag cross-correlation spectrometer backend (GBT/Z; instantaneously covering  $25.6\text{--}36.1\ \text{GHz}$ ; Harris et al. 2007; see Table 1). This yields a typical beam size of  $\sim 23''$ . GBT/S observations were carried out under acceptable to good weather conditions during 14 sessions between 2007 October 10 and 2008 October 12, yielding typical system temperatures of  $T_{\text{sys}}=42\text{--}57\ \text{K}$  (with higher  $T_{\text{sys}}$  toward higher observing frequencies due to the atmosphere). This resulted in  $4.3, 3.7, 2.5$ , and  $8.7\ \text{hr}$  on-source observing time for IRAS F10214+4724, the Cloverleaf, SMM J04135+10277, and MG 0751+2716, respectively. In addition, the Cloverleaf was observed with the GBT/Z for another 6 sessions between 2008 March 02 and 2009 March 12. This resulted in  $14.7\ \text{hr}$  of observing time, about half of which was spent on the Cloverleaf. The GBT/S was configured with  $800\ \text{MHz}$  bandwidth, yielding a spectral resolution of  $391\ \text{kHz}$ . The GBT/Z samples its  $10.5\ \text{GHz}$  bandwidth with  $8\ \text{MHz}$  spectral channels. Its instrumental spectral response is nearly a sinc function with an FWHM of  $20\ \text{MHz}$ , i.e., individual  $8\ \text{MHz}$  spectral channels are not statistically independent. However, the line width correction for the instrumental response for spectral lines with intrinsic Gaussian FWHM of  $>30\ \text{MHz}$  ( $\sim 300\ \text{km s}^{-1}$ ) is minor.

Subreflector beam switching was used every  $10\ \text{s}$  for all observations (GBT/S and GBT/Z) to observe the sources alternately with the receiver’s two beams, with the off-source beam monitoring the sky background in parallel. To remove continuum fluxes and atmospheric/instrumental effects, low-order polynomials were fitted to the spectral baselines of the calibrated, time-averaged GBT/S observations. For the GBT/Z observations, a nearby second, faint source was observed with the same subreflector switching pattern, alternating between targets with  $8\ \text{min}$  cycles. Residual structure from optical beam imbalance in the ‘source-sky’ difference spectra of

TABLE 1  
 OBSERVED CO( $J=1\rightarrow0$ ) LINE PARAMETERS.

| Source       | $z_{\text{CO}}$     | $\mu_L$ | $\nu_{\text{obs}}$<br>[GHz] | $S_\nu$<br>[mJy] | $\Delta V_{\text{FWHM}}$<br>[km s $^{-1}$ ] | $I_{\text{CO}}$<br>[Jy km s $^{-1}$ ] | $L'_{\text{CO}(1\rightarrow0)}{}^a$<br>[ $10^9$ K km s $^{-1}$ pc $^2$ ] | Telescope |
|--------------|---------------------|---------|-----------------------------|------------------|---|---------------------------------------|--|-----------|
| F10214+4724  | $2.2853 \pm 0.0001$ | 17      | 35.0795                     | $2.42 \pm 0.37$  | $169 \pm 39$                                | $0.434 \pm 0.047$                     |  | EVLA      |
|              | $2.2856 \pm 0.0001$ |         |                             | $1.73 \pm 0.22$  | $184 \pm 29$                                | $0.337 \pm 0.045$                     |  | GBT/S     |
|              | $2.2854 \pm 0.0001$ |         |                             |                  |   | $0.383 \pm 0.032$                     | $5.77 \pm 0.49$  | Combined  |
| Cloverleaf   | $2.5564 \pm 0.0004$ | 11      | 32.3992                     | $2.78 \pm 0.40$  | $468 \pm 94$                                | $1.378 \pm 0.250$                     |  | EVLA      |
|              | $2.5578 \pm 0.0001$ |         |                             | $2.72 \pm 0.12$  | $470 \pm 27$                                | $1.358 \pm 0.065$                     |  | GBT/S     |
|              | $2.5574 \pm 0.0001$ |         |                             | $3.14 \pm 0.11$  | $422 \pm 19$                                | $1.406 \pm 0.053$                     |  | GBT/Z     |
|              | $2.5575 \pm 0.0001$ |         |                             |                  |   | $1.387 \pm 0.040$                     | $39.3 \pm 1.1$   | Combined  |
| J0911+0551   | $2.7961 \pm 0.0001$ | 22      | 30.3665                     | $1.75 \pm 0.22$  | $111 \pm 19$                                | $0.205 \pm 0.029$                     | $3.39 \pm 0.48$  | EVLA      |
| J04135+10277 | $2.8470 \pm 0.0004$ | 1.3     | 29.9717                     | $1.20 \pm 0.15$  | $505 \pm 75$                                | $0.644 \pm 0.082$                     | $184 \pm 23$   | GBT/S     |
| MG 0751+2716 | $3.1984 \pm 0.0006$ | 16      | 27.4455                     | $1.61 \pm 0.34$  | $290 \pm 62$                                | $0.494 \pm 0.105$                     |  | EVLA      |
|              | $3.1995 \pm 0.0004$ |         |                             | $1.47 \pm 0.24$  | $354 \pm 72$                                | $0.550 \pm 0.095$                     |  | GBT/S     |
|              | $3.1990 \pm 0.0003$ |         |                             |                  |   | $0.525 \pm 0.070$                     | $14.9 \pm 2.0$   | Combined  |

 NOTE. —  $\mu_L$ : lensing magnification factor (see Riechers 2011, and references therein). GBT/S: Measured with the GBT digital Spectrometer backend. GBT/Z: Measured with the GBT wideband Zpectrometer backend.

<sup>a</sup> Corrected for magnification due to gravitational lensing.

 FIG. 2.— Overlay of CO( $J=1\rightarrow0$ ) and CO( $J=7\rightarrow6$ ) emission (left; CO  $J=7\rightarrow6$  map from Alloin et al. 1997), and independent EVLA, GBT/Spectrometer, and GBT/Zpectrometer CO( $J=1\rightarrow0$ ) spectra (middle left to right) in the Cloverleaf ( $z=2.558$ ). The spectra (histograms) are shown at 4, 3.906, and 8 MHz resolution (37, 36, and 74 km s $^{-1}$ ). The solid curves indicate Gaussian fits to the spectra. The GBT/Z channels are not statistically independent on scales below 20 MHz (2.5 channels).

the two targets was then removed by differencing the resulting spectra of both sources (the second source was not detected). This strategy yields a flat baseline (offset from zero flux by the difference of the two source's continua) without standard polynomial baseline removal. For all observations, several nearby quasars were targeted regularly to monitor telescope pointing and gain stability. Passband gains and absolute fluxes for all observations were determined from spectra of 3C286 and 3C147, yielding 10%–15% calibration accuracy.

All data were processed with GBTIDL (Marganian et al. 2006), using standard recipes and/or the Zpectrometer's data reduction pipeline (see Harris et al. 2010 for GBT/Z details). After processing, the GBT/S data were re-binned to 3.906 MHz (33–43 km s $^{-1}$ ) for further analysis.

### 3. RESULTS

We have detected strong CO( $J=1\rightarrow0$ ) emission toward IRAS F10214+4724, the Cloverleaf, RX J0911+0551, SMM J04135+10277, and MG 0751+2716. We spatially resolve the CO( $J=1\rightarrow0$ ) emission in IRAS F10214+4724 and the Cloverleaf, but do not resolve the CO( $J=1\rightarrow0$ ) emission in RX J0911+0551 and MG 0751+2716 (Fig. 1). The measured sizes and upper limits are consistent with the lens configurations of these targets if the CO reservoirs have intrinsic sizes of a few kpc. Accounting for beam convolution, the gas distribution in the Cloverleaf is consistent with that observed in higher- $J$  lines

(e.g., Alloin et al. 1997), but may be somewhat more extended (Fig. 2, left). We detect rest-frame 2.6 mm continuum emission toward the Cloverleaf and MG 0751+2716 at  $386 \pm 107 \mu\text{Jy}$  and  $17.4 \pm 0.7 \text{ mJy}$  strength. We also detect rest-frame 2.2 mm continuum emission toward MG 0751+2716 at  $13.9 \pm 0.6 \text{ mJy}$  strength. We do not detect rest-frame 2.6 mm continuum emission toward IRAS F10214+4724 and RX J0911+0551 down to  $3\sigma$  limits of 270 and 170  $\mu\text{Jy}$ . The continuum emission in MG 0751+2716 is consistent with non-thermal emission from its radio-loud AGN (e.g., Lehar et al. 1997; Riechers et al. 2006b). The continuum detection and limits for the other targets are consistent with thermal and non-thermal emission associated with star formation in their host galaxies (e.g., Weiß et al. 2003; Ao et al. 2008; Wu et al. 2009).

The CO( $J=1\rightarrow0$ ) line profiles of all sources were fitted with single-component Gaussians, which yields good fits to all data (Figs. 2 and 3). The three independent measurements of the CO( $J=1\rightarrow0$ ) line in the Cloverleaf (EVLA, GBT/S, and GBT/Z) yield consistent line profiles and intensities within the relative uncertainties, suggesting that the interferometric observations recover the full flux, and that the calibration of the single-dish observations is reliable to high accuracy. Due to the limited bandwidth of the observations of RX J0911+0551, the line is only marginally covered in velocity. However, the fitted line FWHM of  $111 \pm 19 \text{ km s}^{-1}$  is in excellent agreement with the  $\sim 110 \text{ km s}^{-1}$  measured in the

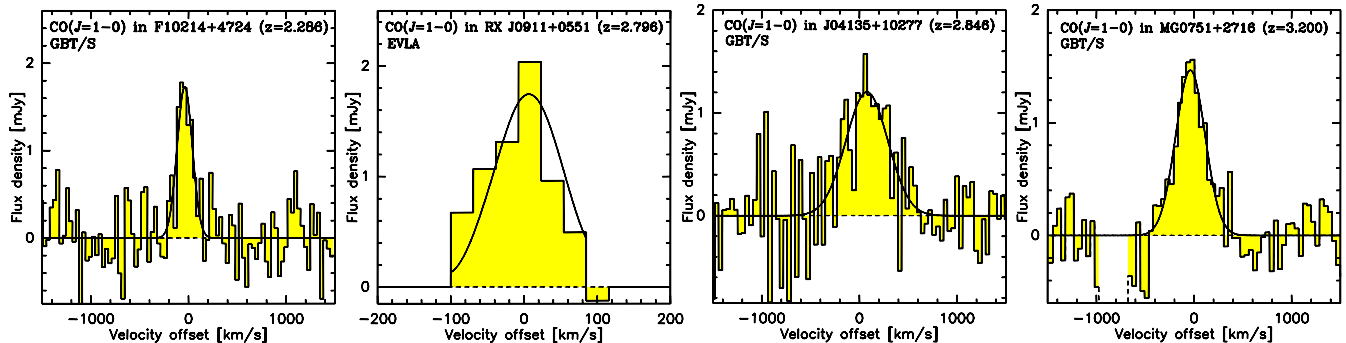


FIG. 3.— EVLA and GBT/Spectrometer spectra of CO( $J=1\rightarrow0$ ) emission toward IRAS F10214+4724 ( $z=2.286$ ), RX J0911+0551 ( $z=2.796$ ), SMM J04135+10277 ( $z=2.846$ ), and MG 0751+2716 ( $z=3.200$ ). The spectra (histograms) are shown at 3.906 MHz resolution ( $33\text{--}43\text{ km s}^{-1}$ ), except RX J0911+0551, which is shown at 3.125 MHz ( $31\text{ km s}^{-1}$ ) resolution. The solid curves indicate Gaussian fits to the spectra. The blanked-out region in the spectrum of MG 0751+2716 masks a resonance from the GBT Ka band receiver’s feeds.

CO( $J=3\rightarrow2$ ) to CO( $J=9\rightarrow8$ ) lines (A. Weiß et al., in prep.).<sup>10</sup> The GBT/S measurement of the CO( $J=1\rightarrow0$ ) line in MG 0751+2716 shows an instrumental resonance feature  $\sim 800\text{ km s}^{-1}$  blueswards from the line center, which is excluded from the spectral baseline fit, and does not appear to affect the line flux measurement. The CO( $J=1\rightarrow0$ ) line peak flux densities, widths, integrated intensities, and centroid redshifts for all sources and measurements are detailed in Table 1. Two or three independent CO( $J=1\rightarrow0$ ) measurements were obtained for IRAS F10214+4724, the Cloverleaf, and MG 0751+2716. The median CO redshifts and line intensities for these sources are given in Table 1, and are adopted for all further analysis. All five targets are gravitationally lensed. Based on the CO( $J=1\rightarrow0$ ) line intensities and lensing magnification factors from the literature (see Riechers 2011, and references therein), we derive lensing-corrected CO( $J=1\rightarrow0$ ) line luminosities of  $L'_{\text{CO}(1-0)} = 0.34 - 18.4 \times 10^{10}\text{ K km s}^{-1}\text{ pc}^2$  (Tab. 1).

Our CO( $J=1\rightarrow0$ ) fluxes imply CO( $J=3\rightarrow2$ )/CO( $J=1\rightarrow0$ ) line brightness temperature ratios<sup>11</sup> of  $r_{31}=T_b^{\text{CO}(3-2)}/T_b^{\text{CO}(1-0)}=1.00\pm0.10$ ,  $1.06\pm0.03$ ,  $\sim 0.95$ ,  $0.93\pm0.25$ , and  $0.97\pm0.17$  for IRAS F10214+4724, the Cloverleaf, RX J0911+0551, SMM J04135+10277, and MG 0751+2716, respectively (CO  $J=3\rightarrow2$  measurements are from Ao et al. 2008, Weiß et al. 2003, A. Weiß et al., in prep., Hainline et al. 2004, and Alloin et al. 2007, respectively). These values are fully consistent with thermalized gas excitation (i.e.,  $r_{31}=1$ ) in all targets.

#### 4. ANALYSIS

##### 4.1. Line Excitation Modeling

The two best-studied targets in our sample are IRAS F10214+4724 and the Cloverleaf (e.g., Ao et al. 2008; Barvainis et al. 1997; Weiß et al. 2003; Bradford et al. 2009). Based on CO( $J=3\rightarrow2$ ) to CO( $J=9\rightarrow8$ ) observations in the literature and our CO( $J=1\rightarrow0$ ) detections, we can constrain the line radiative transfer through Large Velocity Gradient (LVG) models, treating the gas kinetic temperature and density as free parameters. For all calculations, the H<sub>2</sub> ortho-to-para ra-

tio was fixed to 3:1, the cosmic microwave background temperature was fixed to 8.95 and 9.69 K (at  $z=2.286$  and 2.558), and the Flower (2001) CO collision rates were used. For consistency with previous modeling of both sources (Ao et al. 2008; Riechers et al. 2011a), we adopted a CO abundance per velocity gradient of  $[\text{CO}]/(dv/dr) = 1 \times 10^{-5}\text{ pc (km s}^{-1})^{-1}$  (e.g., Weiß et al. 2005, 2007; Riechers et al. 2006a).

Observations of both targets are fit very well by single-component models (except the CO  $J=5\rightarrow4$  flux in the Cloverleaf, which is likely too low due to calibration issues related to the restricted bandwidth of these early observations; Barvainis et al. 1997; see also A. Weiß et al., in prep.). For IRAS F10214+4724, we fit a representative model with a kinetic gas temperature of  $T_{\text{kin}}=60\text{ K}$  and a gas density of  $\rho_{\text{gas}}=10^{3.8}\text{ cm}^{-3}$ , yielding a moderate optical depth of  $\tau_{\text{CO}(1-0)}=1.6$  (Fig. 4a and c). For the Cloverleaf, we fit a representative model with  $T_{\text{kin}}=50\text{ K}$  and  $\rho_{\text{gas}}=10^{4.5}\text{ cm}^{-3}$ , yielding a high optical depth of  $\tau_{\text{CO}(1-0)}=8.9$  (Fig. 4b and d). While not formally excluding the presence of some colder gas (given the remaining uncertainties), these models are consistent with previous fits based on the CO  $J\geq 3$  transitions alone (Ao et al. 2008; Bradford et al. 2009; Riechers et al. 2011a). They are also consistent with what is found for  $z>4$  quasars observed in CO( $J=1\rightarrow0$ ) emission (Riechers et al. 2006a; Weiß et al. 2007). This finding is in agreement with the CO( $J=1\rightarrow0$ ) emission in high- $z$  quasars being associated with optically thick emission from the highly excited molecular gas detected in high- $J$  CO transitions, without any evidence for significant additional low-excitation gas components.

##### 4.2. Molecular Gas Masses

The CO( $J=1\rightarrow0$ ) emission in our targets appears to be associated with highly excited gas that has physical properties consistent with those found in the nuclei of nearby ultra-luminous infrared galaxies (ULIRGs). We thus calculate their gas masses assuming a ULIRG-like conversion factor of  $\alpha_{\text{CO}}=0.8\text{ }M_{\odot} (\text{K km s}^{-1}\text{ pc}^2)^{-1}$  from  $L'_{\text{CO}(1-0)}$  to  $M_{\text{gas}}$  (Downes & Solomon 1998). This yields lensing-corrected molecular gas masses of  $M_{\text{gas}}=0.46$ , 3.1, 0.27, 14.7, and  $1.2 \times 10^{10}\text{ }M_{\odot}$  for IRAS F10214+4724, the Cloverleaf, RX J0911+0551, SMM J04135+10277, and MG 0751+2716, respectively. SMM J04135+10277 is now revealed as the high- $z$  quasar with the highest  $M_{\text{gas}}$  currently known. The gas masses of all systems lie within

<sup>10</sup> These measurements revise the CO( $J=3\rightarrow2$ ) line flux and width measured by Hainline et al. 2004 down by  $\sim 40\%$  and by a factor of  $\sim 3$ , respectively.

<sup>11</sup> The error bars for  $r_{31}$  are derived from the statistical uncertainties of the CO( $J=1\rightarrow0$ ) and CO( $J=3\rightarrow2$ ) measurements.

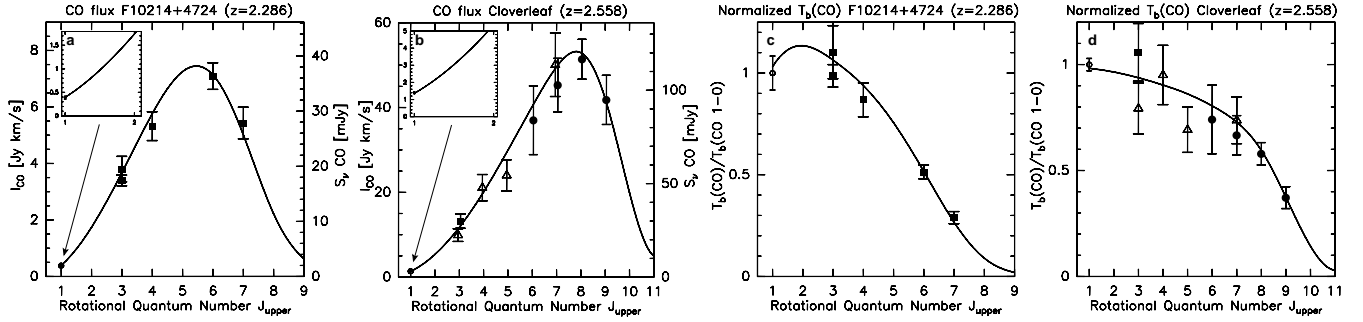


FIG. 4.— CO excitation ladders (points) and LVG models (lines) for IRAS F10214+4724 (panels a and c) and the Cloverleaf (panels b and d), scaled by CO intensity (left two panels) and normalized brightness temperature  $T_b$  (right two panels). The insets show zoomed-in versions of the model fits close to the CO( $J=1\rightarrow0$ ) line. The CO data for IRAS F10214+4724 (circle: this work; squares: Ao et al. 2008) and the Cloverleaf (circle: this work; triangles: Barvainis et al. 1997; filled square: Weiß et al. 2003; filled circles: Bradford et al. 2009; error bars of literature data have been conservatively extended to include 10%–15% calibration uncertainties) are fit well by single, highly excited gas components with kinetic temperatures of  $T_{\text{kin}}=60$  and 50 K and gas densities of  $\rho_{\text{gas}}=10^{3.8}$  and  $10^{4.5} \text{ cm}^{-3}$ , respectively (see also Ao et al. 2008; Riechers et al. 2011a).

the range found for other high- $z$  quasars (mostly determined based on observations of  $J\geq3$  CO transitions), with IRAS F10214+4724 and RX J0911+0551 being situated at the low end of the observed range (which can currently only be investigated with the aid of strong gravitational lensing; e.g., Riechers 2011).

## 5. DISCUSSION AND CONCLUSIONS

We have detected strong CO( $J=1\rightarrow0$ ) emission toward IRAS F10214+4724 ( $z=2.286$ ), the Cloverleaf ( $z=2.558$ ), RX J0911+0551 ( $z=2.796$ ), SMM J04135+10277 ( $z=2.846$ ), and MG 0751+2716 ( $z=3.200$ ). Our EVLA observations have spatially resolved the emission toward IRAS F10214+4724 and the Cloverleaf (Fig. 1). We find line brightness temperatures consistent with those measured in mid- $J$  CO lines. Excitation modeling indicates that the CO( $J=1\rightarrow0$ ) emission is associated with the warm, highly excited gas in the star-forming regions in the host galaxies that is also seen in the higher- $J$  CO lines. This result suggests that mid- $J$  CO lines are good indicators of the total amount of molecular gas in gas-rich high redshift quasar host galaxies, consistent with previous findings based on a smaller sample of  $z\gtrsim4$  quasars (Riechers et al. 2006a), and extending these studies to the peak epoch of cosmic star formation and AGN activity. In contrast, recent studies of CO( $J=1\rightarrow0$ ) emission in  $z>2$  SMGs suggest that many of these galaxies have substantial amounts of low-excitation gas (e.g., Hainline et al. 2006; Carilli et al. 2010; Harris et al. 2010; Ivison et al. 2010, 2011; Riechers et al. 2010, 2011b, 2011c). Such a difference is in agreement with the picture that gas-rich quasars and SMGs represent different stages in the early evolution of massive galaxies. Such an observational finding would be consistent with a high redshift analogue of the ULIRG-quasar transition scenario proposed by Sanders et al. (1988).

In this picture, it may be expected to find some sources with gas properties that overlap with both populations, i.e., SMGs with molecular gas properties closer to those

of the quasars studied here. The recently identified  $z=2.957$  SMG HLSW-01 may be an example of such “overlap” sources. Most of its gas properties are consistent with those of “typical” SMGs (i.e., its gas mass, gas mass fraction, gas depletion timescale, star formation efficiency, specific star formation rate, and dynamical structure; Riechers et al. 2011d), but it shows a high  $r_{31}=0.95\pm0.10$  (i.e., consistent with 1), and an overall high CO excitation (Riechers et al. 2011d; Scott et al. 2011). Its high radio luminosity, dust temperature, and CO excitation may suggest the presence of a luminous, perhaps obscured AGN (Conley et al. 2011; Riechers et al. 2011d; Scott et al. 2011). However, based on CO studies at high  $z$  to date, systems like HLSW-01 appear to be rare among SMGs.

These results demonstrate that observations of low-order CO transitions in high redshift galaxies with the EVLA will be of enormous utility to establish the context for studies of highly excited CO emission with the Atacama Large (sub)millimeter Array (ALMA). Complementary studies with the EVLA and ALMA will be key to distinguishing different high- $z$  galaxy populations based on the physical properties of the molecular gas in their star-forming environments.

This letter is dedicated to the memory of Phil Solomon. His contributions to the field were a true inspiration, and we gratefully acknowledge his wisdom in the early discussions of the GBT program. We thank the referee, Dr. Philip Maloney, for a helpful report. We thank Charles C. Figura for assistance in the development of data reduction techniques related to the GBT Spectrometer observations. We thank Christian Henkel for the original version of the LVG code. DR acknowledges support from NASA through a Spitzer Space Telescope grant. AJB acknowledges support from NSF grant AST-0708653 to Rutgers University. The National Radio Astronomy Observatory is a facility of the National Science Foundation operated under cooperative agreement by Associated Universities, Inc.

## REFERENCES

- Alloin, D., Guilloteau, S., Barvainis, R., Antonucci, R., & Tacconi, L., 1997, A&A, 321, 24
- Alloin, D., Kneib, J.-P., Guilloteau, S., & Bremer, M. 2007, A&A, 470, 53
- Ao, Y., et al. 2008, A&A, 491, 747
- Barvainis, R., Maloney, P., Antonucci, R., & Alloin, D. 1997, ApJ, 484, 695
- Blain, A. W., et al. 2002, PhR, 369, 111
- Bradford, C. M., et al. 2009, ApJ, 705, 112
- Carilli, C. L., et al. 2002, ApJ, 575, 145

- Carilli, C. L., Daddi, E., Riechers, D., et al. 2010, *ApJ*, 714, 1407
- Conley, A., et al. 2011, *ApJ*, 732, L35
- Downes, D., & Solomon, P. M. 1998, *ApJ*, 507, 615
- Flower, D. R. 2001, *J. Phys. B: At. Mol. Opt. Phys.*, 34, 2731
- Greve, T. R., et al. 2005, *MNRAS*, 359, 1165
- Hainline, L. J., Scoville, N. Z., Yun, M. S., Hawkins, D. W., Frayer, D. T., & Isaak, K. G. 2004, *ApJ*, 609, 61
- Hainline, L. J., Blain, A. W., Greve, T. R., Chapman, S. C., Smail, I., & Ivison, R. J. 2006, *ApJ*, 650, 614
- Harris, A. I., et al. 2007, in *From Z-Machines to ALMA: (Sub)Millimeter Spectroscopy of Galaxies*, ed. A. J. Baker, J. Glenn, A. I. Harris, J. G. Mangum, & M. S. Yun (San Francisco: ASP), 82
- Harris, A. I., Baker, A. J., Zonak, S. G., Sharon, C. E., Genzel, R., Rauch, K., Watts, G., & Creager, R. 2010, *ApJ*, 723, 1139
- Ivison, R. J., et al. 2010, *MNRAS*, 404, 198
- Ivison, R. J., Papadopoulos, P. P., Smail, I., Greve, T. R., Thomson, A. P., Xilouris, E. M., & Chapman, S. C. 2011, *MNRAS*, 412, 1913
- Lehár, J., et al. 1997, *AJ*, 114, 48
- Magnelli, B., Elbaz, D., Chary, R. R., Dickinson, M., Le Borgne, D., Frayer, D. T., & Willmer, C. N. A. 2009, *A&A*, 496, 57
- Marganian, P., Garwood, R. W., Braatz, J. A., Radziwill, N. M., & Madaena, R. J. 2006, in *Astronomical Data Analysis Software and Systems XV*, ed. C. Gabriel, C. Arviset, D. Ponz, & Enrique Solano (San Francisco: ASP), 512
- Perley, R. A., Chandler, C. J., Butler, B. J., & Wrobel, J. M. 2011, *ApJL*, in press (arXiv:1106.0532)
- Richards, G. T., et al. 2006, *AJ*, 131, 2766
- Riechers, D. A., et al. 2006a, *ApJ*, 650, 604
- Riechers, D. A., et al. 2006b, *ApJ*, 649, 635
- Riechers, D. A., et al. 2010, *ApJ*, 720, L131
- Riechers, D. A., 2011, *ApJ*, 730, 108
- Riechers, D. A., et al. 2011a, *ApJ*, 726, 50
- Riechers, D. A., et al. 2011b, *ApJL*, in press (arXiv:1105.4177)
- Riechers, D. A., et al. 2011c, *ApJ*, 733, L11
- Riechers, D. A., et al. 2011d, *ApJ*, 733, L12
- Sanders, D. B., Soifer, B. T., Elias, J. H., Madore, B. F., Matthews, K., Neugebauer, G., & Scoville, N. Z. 1988, *ApJ*, 325, 74
- Scott, K., et al. 2011, *ApJ*, 733, 29
- Solomon, P. M., & Vanden Bout, P. A. 2005, *ARA&A*, 43, 677
- Spergel, D. N., et al. 2003, *ApJS*, 148, 175
- Spergel, D. N., et al. 2007, *ApJS*, 170, 377
- Wei, A., Henkel, C., Downes, D., & Walter, F. 2003, *A&A*, 409, L41
- Wei, A., Walter, F., & Scoville, N. Z. 2005, *A&A*, 438, 533
- Wei, A., et al. 2007, *A&A*, 467, 955
- Wu, J., Vanden Bout, P. A., Evans, N. J., & Dunham, M. M. 2009, *ApJ*, 707, 988